

Electronic Supplementary Information (ESI)

Hyaluronic acid conjugated polydopamine functionalized mesoporous silica nanoparticles for synergistic targeted chemo- photothermal therapy

Chao Chen^{a†}, Wen Tang^{a†}, Dawei Jiang^b, Guoliang Yang^b, Xiaoli Wang^a, Lina
Zhou^a, Weian Zhang^{b,*}, Ping Wang^{a,c,*}

^aState Key Laboratory of Bioreactor Engineering, Biomedical Nanotechnology Center,
School of Biotechnology, East China University of Science and Technology, Shanghai
200237 (China).

^bShanghai Key Laboratory of Functional Materials Chemistry, East China University
of Science and Technology, 130 Meilong Road, Shanghai 200237 (China).

^cDepartment of Bioproducts and Biosystems Engineering, University of Minnesota, St
Paul, MN 55108, USA.

*Corresponding authors:

Prof. Weian Zhang: E-mail: wazhang@ecust.edu.cn

Prof. Ping Wang: E-mail: pwang11@ecust.edu.cn; ping@umn.edu

†These authors contributed equally.

Cell culture

Hela and L-02 cells were cultured in RPMI 1640 supplemented with 10% fetal bovine serum and antibiotics (100 µg/mL streptomycin and 100 U/mL penicillin) in 5% CO₂ at 37°C. Media in all samples were changed every two days and the cells were separated by trypsin before cell density reached 80%.

Hemolysis assay

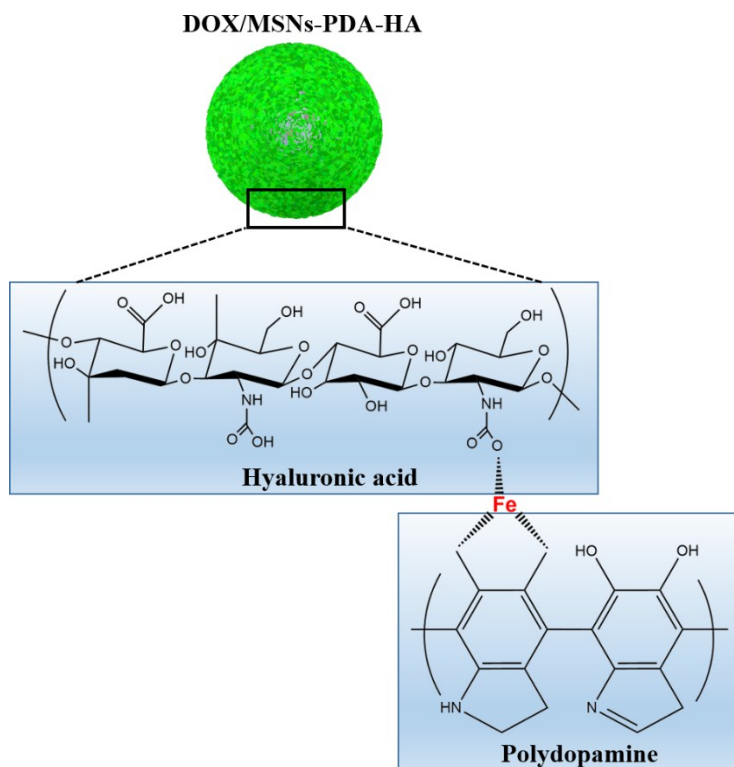
Hemolysis assay was employed to evaluate the safety of the MSNs and MSN-PDA-HA for intravenous injection[1]. The human red blood cells (RBCs) were harvested at 1000 r/min for 10 min and washed with PBS for three times. Then the RBCs were diluted to a concentration of 2 % (v:v). Then, 2 ml of the suspension saline solutions of MSNs and MSNs-PDA-HA samples were added into the equal volume of 2 % RBCs solutions, and the final concentrations of the samples were 10, 20, 50, 100, 200, 400 and 500 µg/ml. The mixtures were shaken (100 rpm) at 37°C for 4 h. Then, the mixtures were centrifuged for 10 min at 1800 r/min and the upper clear solutions were taken out and measured at 541 nm on a UV-vis spectrophotometer. The hemolysis of RBCs in distilled water and saline was used as the positive and negative control, respectively.

Hemolysis percentages (%) = (absorbances of the sample - absorbances of the negative control) / (absorbances of the positive - absorbances of negative control) × 100

BSA adsorption measurements

The protein adsorption onto the surface of silica nanoparticles was simulated by BSA adsorption studies according to the published method[1, 2]. BSA (60 mg) was dissolved in distilled water (100 mL) under mild shaking. 10 mg MSNs, MSNs-PDA and MSNs-PDA-HA were respectively dispersed into 5 mL PBS solution, and then 5 mL BSA solution was added. The mixture was placed in a shaker with a shaking rate of 135 rpm at 37°C. After shaking for 4h, the mixture was centrifuged and upper clear solution was collected. Finally, the BSA clear solution was stained with Coomassie brilliant blue solution and measured at 595 nm. BSA adsorbed on MSNs, MSNs-PDA and MSNs-PDA-HA were calculated using following equation:

$q=(C_i-C_f)V/m$, where q is the BSA adsorbance; C_i and C_f are the initial and final BSA concentrations in solutions, respectively; V is the total solution volume; m is the weight of silica nanoparticles added into the solution.



Scheme S1. A schematic diagram for the Fe^{3+} -mediated coordination interaction between hyaluronic acid (HA) and polydopamine (PDA).

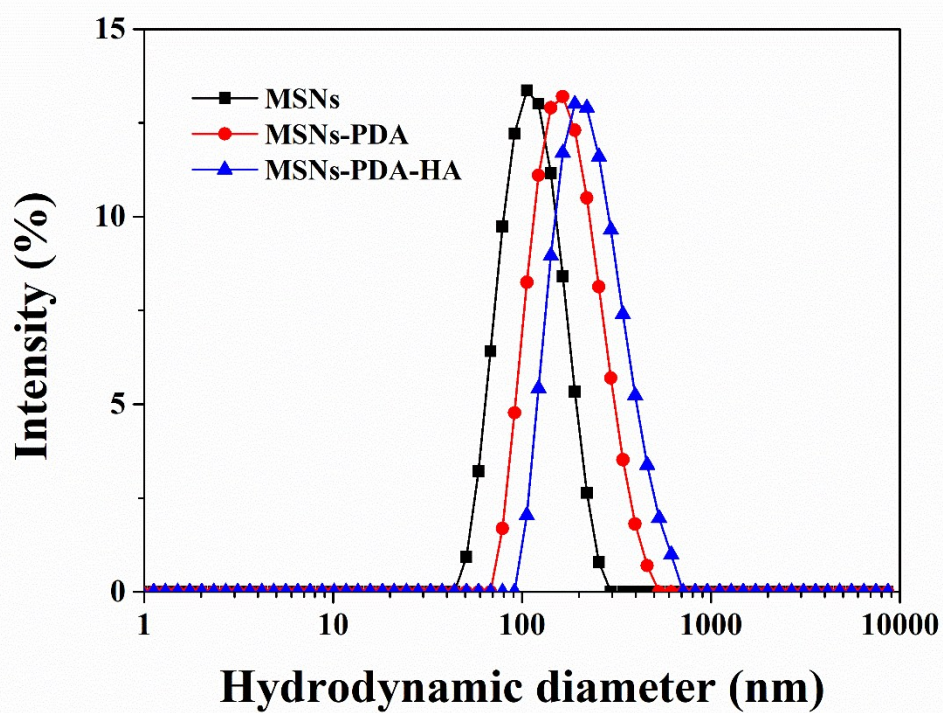


Fig. S1. Hydrodynamic particle size of MSNs, MSNs-PDA and MSNs-PDA-HA in water.

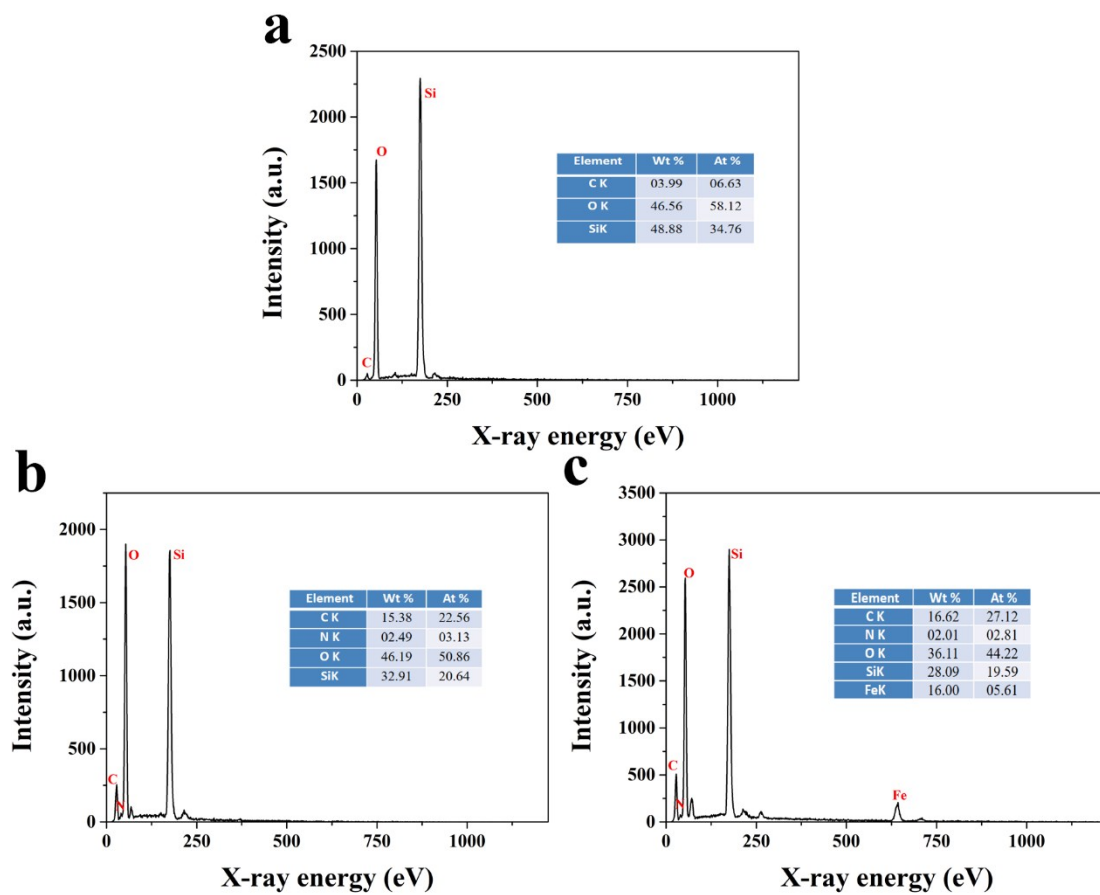


Fig. S2. The corresponding energy dispersive X-ray (EDX) spectra and the element analysis of (a) MSNs, (b) MSNs-PDA and (c) MSNs-PDA-HA.

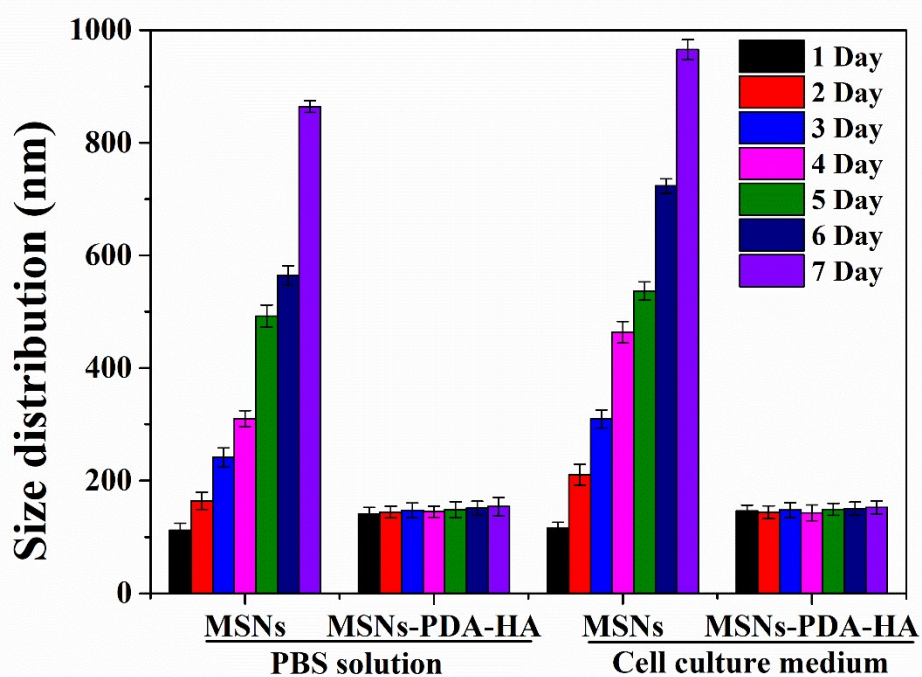


Fig. S3. Stability of MSNs-PDA-HA in PBS (pH 7.4) and cell culture media (RPMI 1640 containing 10% FBS).

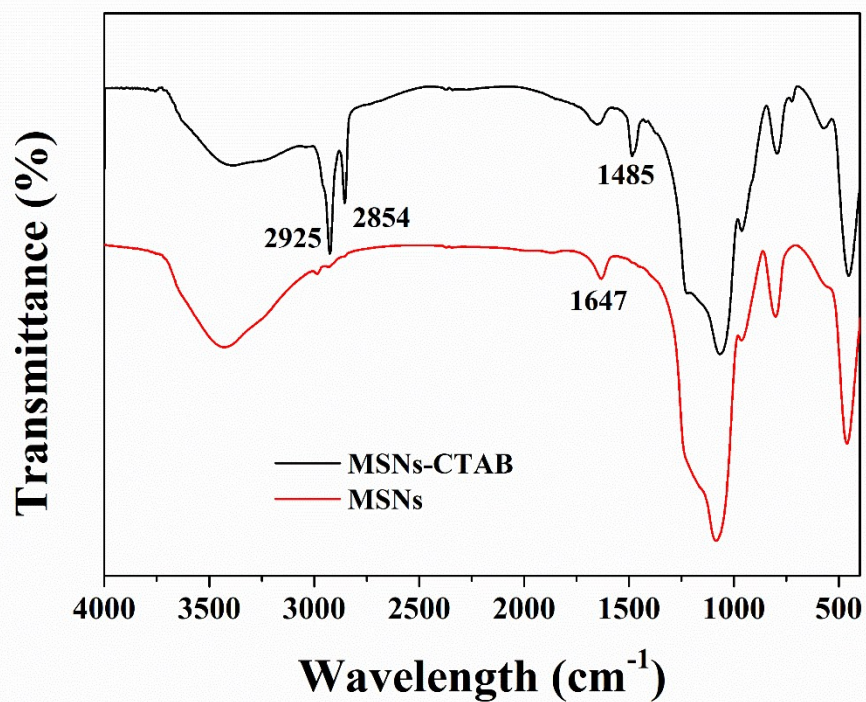


Fig. S4. FTIR spectra of MSNs and MSNs-CTAB. The appearance of peaks appeared at 2925 and 2854 cm^{-1} attributed to the characteristic C-H deformation vibration and the peaks at about 1485 cm^{-1} assigned C-H deformation vibration due to large amount of CTAB in the channels confirmed the structure of MSN-CTAB.

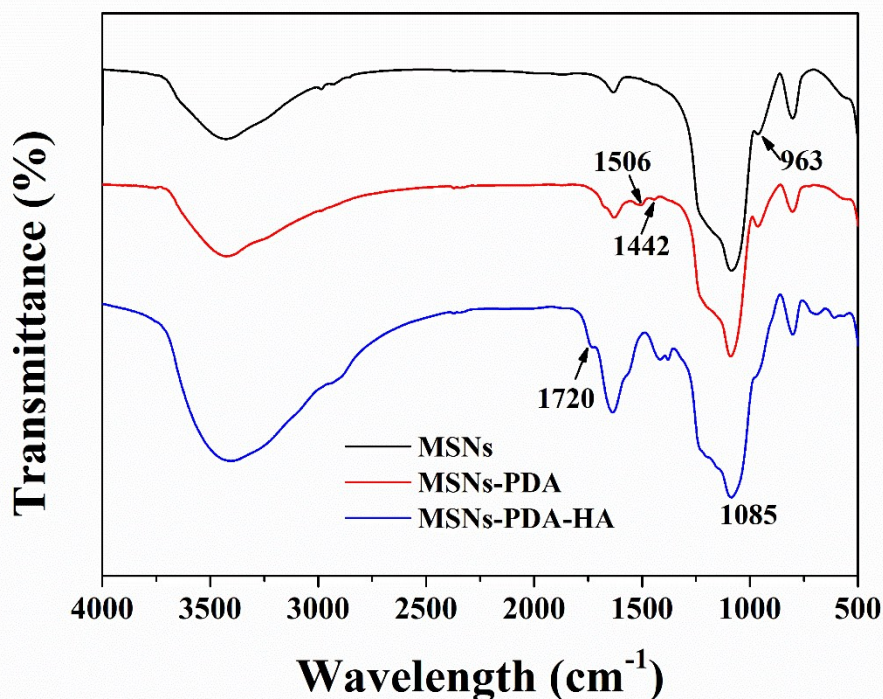


Fig. S5. FTIR spectra of MSNs, MSNs-PDA and MSNs-PDA-HA. The spectra of all samples displayed peaks at 1085 and 963 cm^{-1} , which are the Si-O-Si stretching vibration and silanol group vibration, respectively. After coating with PDA, several new absorption signals appeared. The absorption peaks at 1506 and 1442 cm^{-1} were caused by the overlap of the C=C resonance vibrations in the aromatic ring and the N-H bending vibrations. These characteristic absorption bands were all from PDA layers, indicating the successful incorporation of the PDA layer on the surface of MSNs. After modification with HA, distinctive absorption peak at 1720 cm^{-1} (C=O) was observed when comparing with that of MSNs-PDA. The results indicated that HA was successfully conjugated to MSNs-PDA.

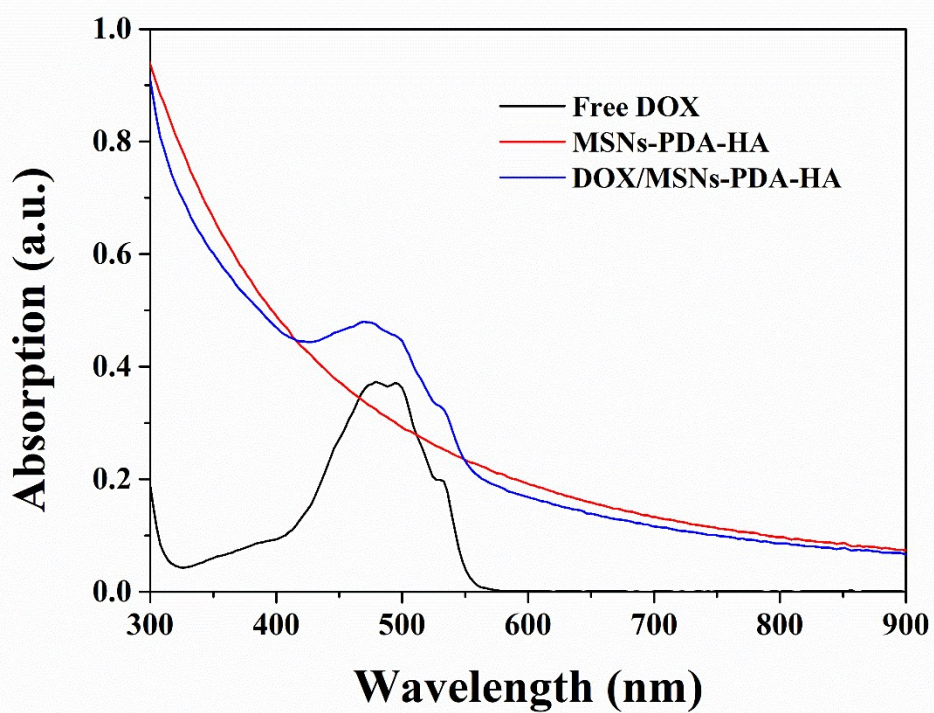


Fig. S6. UV-vis absorption spectra of Free DOX, MSNs-PDA-HA and DOX/MSNs-PDA-HA nanocomposites dispersed in water.

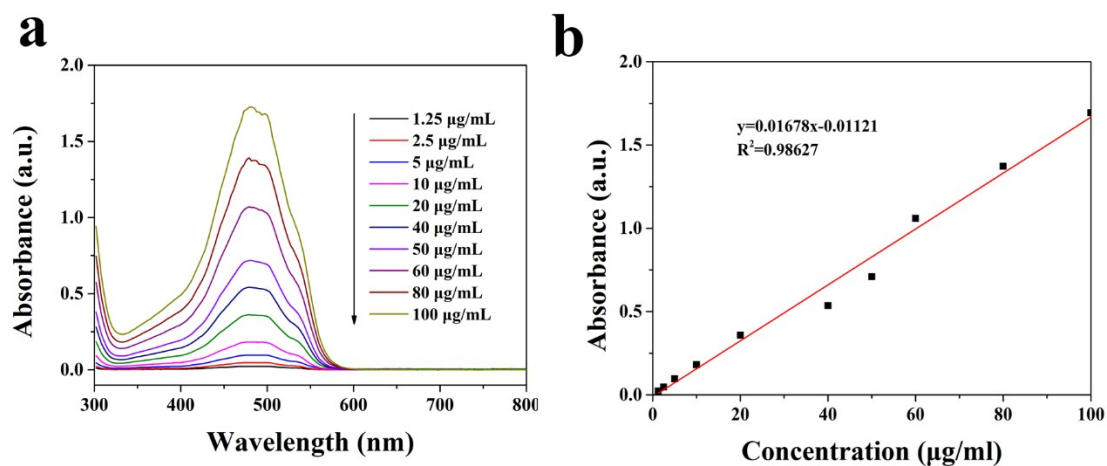


Fig. S7. (a) The absorption spectra of DOX with different concentrations. (b) The standard curve of DOX absorbance value at 488 nm. The obtained standard curve is $y=0.01678x+0.01121$ (Y: absorbance value at 488 nm; X: concentration of DOX, $R^2=0.98627$).

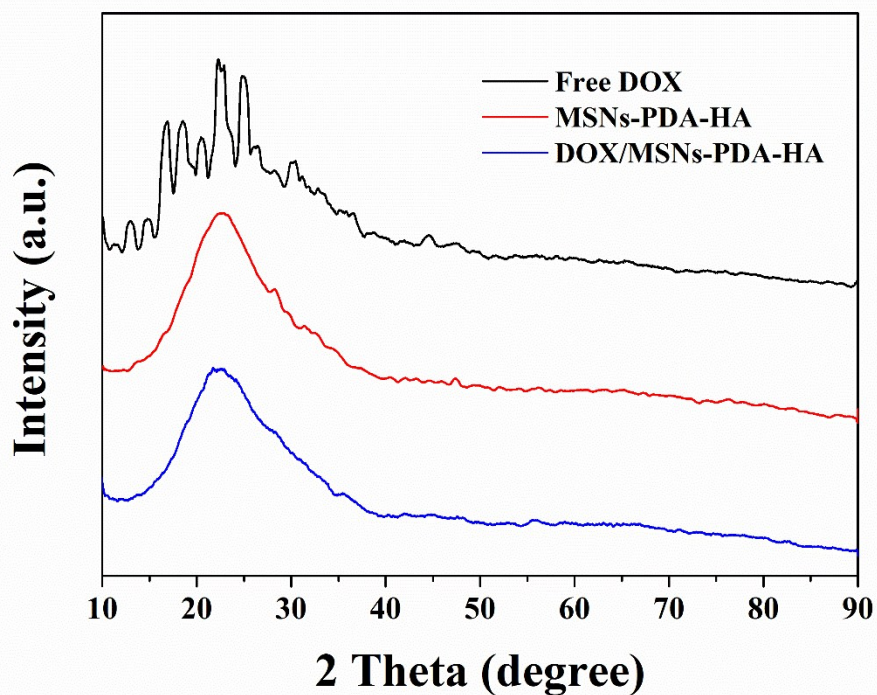


Fig. S8. XRD patterns of Free DOX, MSNs-PDA-HA and DOX/MSNs-PDA-HA nanocomposites.

The crystalline properties of free DOX, MSNs-PDA-HA and DOX/MSNs-PDA-HA samples were evaluated by XRD. As shown in Fig. S8, free DOX showed intense and characteristic crystalline diffraction peaks. However, no distinctive crystalline peaks were found in the MSNs-PDA-HA and DOX/MSNs-PDA-HA samples. These results confirmed that the existing state of DOX in MSNs-PDA-HA was in a non-crystalline state due to the confined effect of the mesopore of the silica.

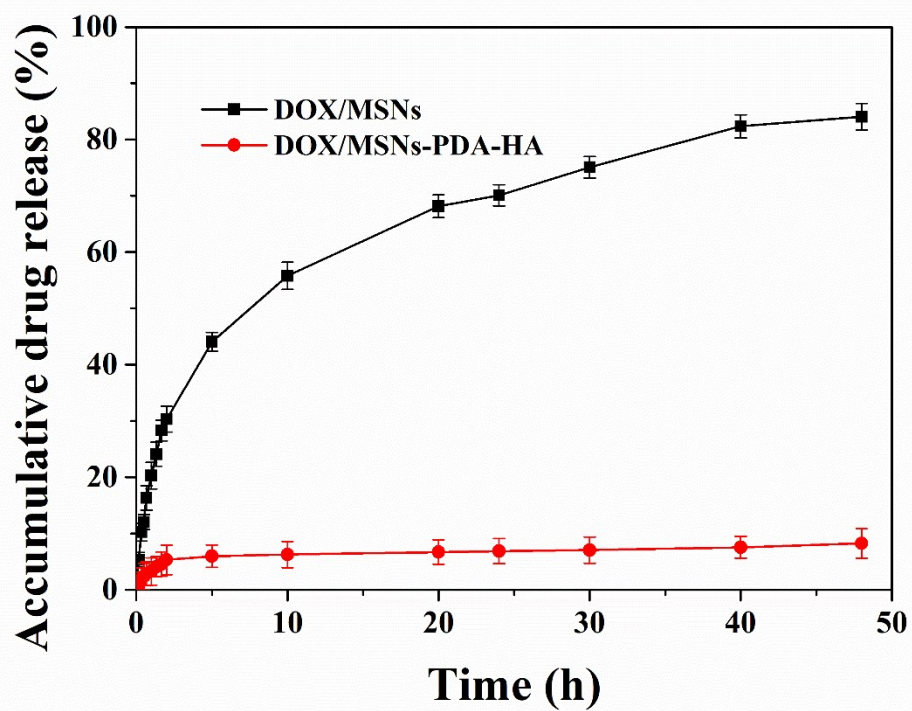


Fig. S9. DOX release from DOX/MSNs and DOX/MSNs-PDA-HA in PBS (pH=7.4). Data are represented as mean \pm SD (n = 3).

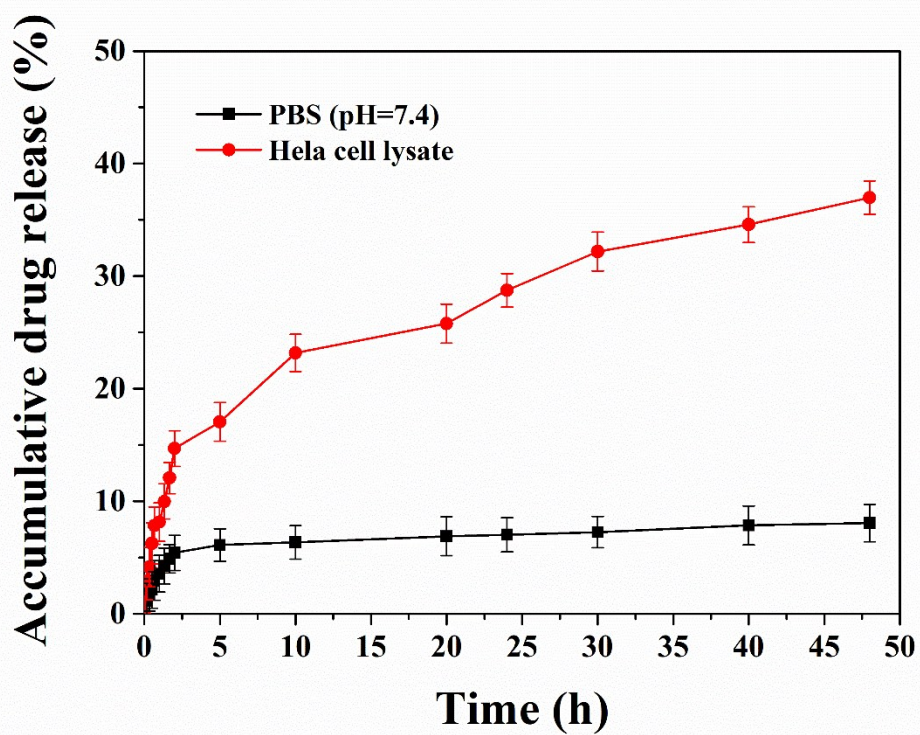


Fig. S10. *In vitro* release profiles of DOX/MSNs-PDA-HA in HeLa cell lysate and PBS (pH=7.4). Data are represented as mean \pm SD (n = 3).

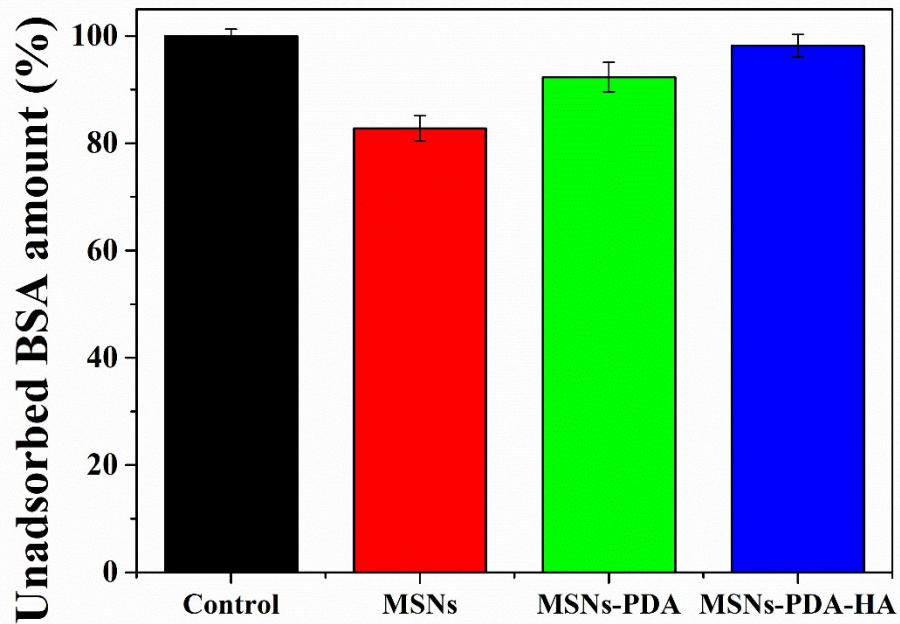


Fig. S11. Unadsorbed BSA amount of MSNs, MSNs-PDA and MSNs-PDA-HA. Data are represented as mean \pm SD (n = 3).

The adsorption of BSA to the surface of MSNs, MSNs-PDA and MSNs-PDA-HA was measured to prove the effectiveness of HA modification. MSNs and MSNs-PDA had a considerable BSA adsorbance of 17.22 and 7.66 wt%, while the adsorbance of BSA to MSNs-PDA-HA surface sharply decreased to about 1.8 wt%. This result confirmed that HA capping could protect MSNs effectively from nonspecific protein adsorption.

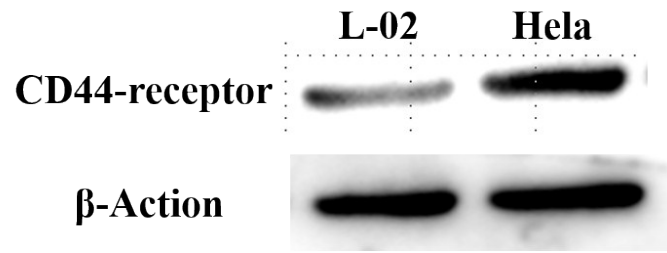


Fig. S12. Western blot showing the distinct expressing of CD44-receptor in L-02 and HeLa cells.

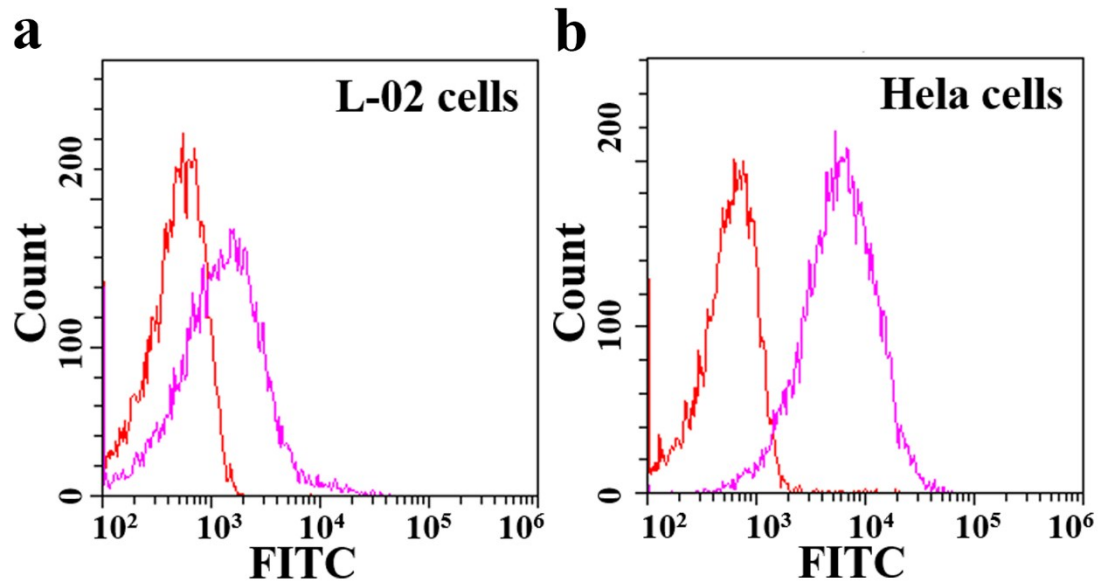


Fig. S13. Flow cytometry quantification of the CD44-receptor expression level in (a) L-02 and (b) HeLa cells.

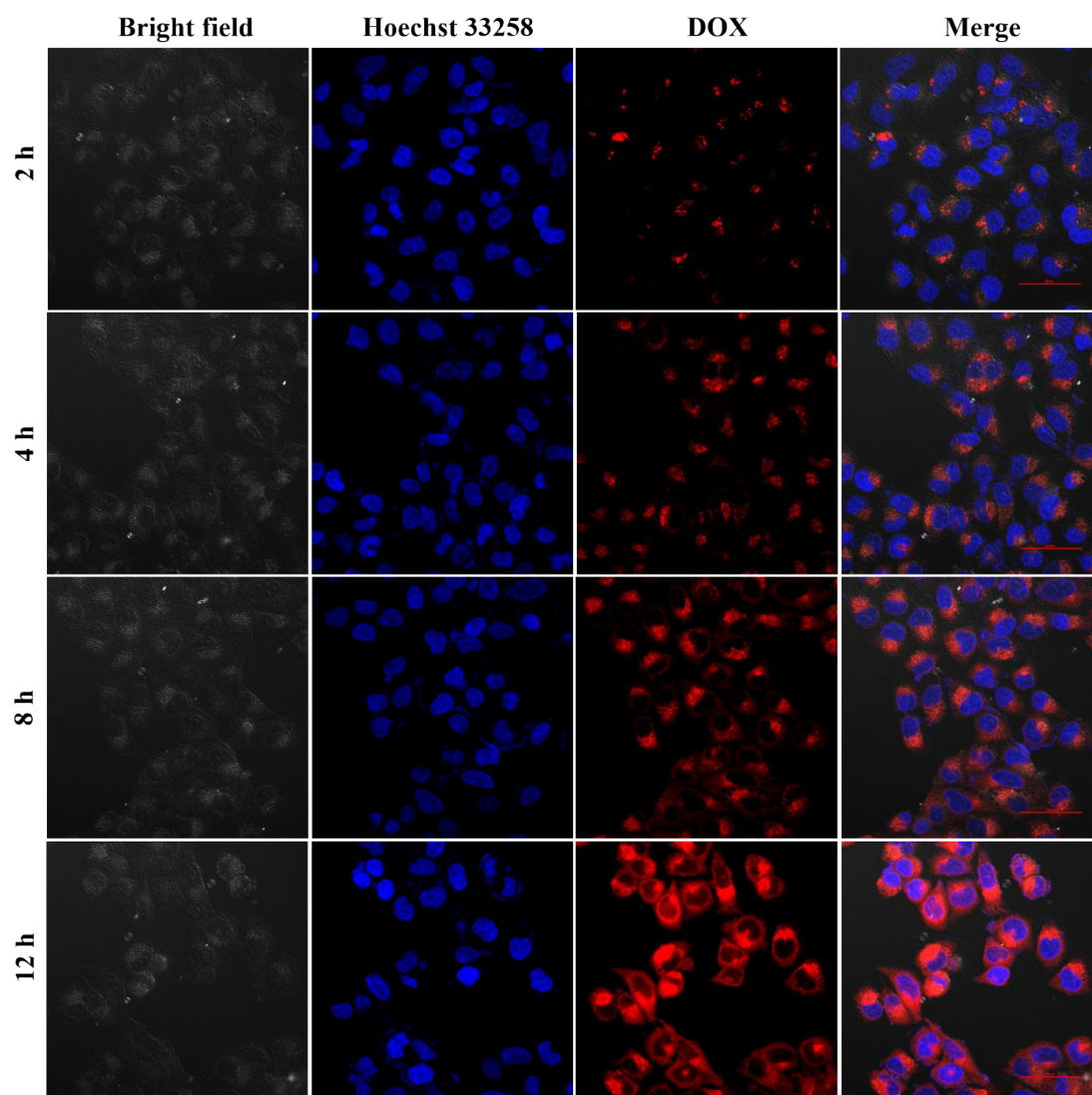


Fig. S14. CLSM images of HeLa cells incubated with DOX/MSNs-PDA-HA for 2 h, 4 h, 8 h and 12 h, respectively. Scale bar: 50 μm .

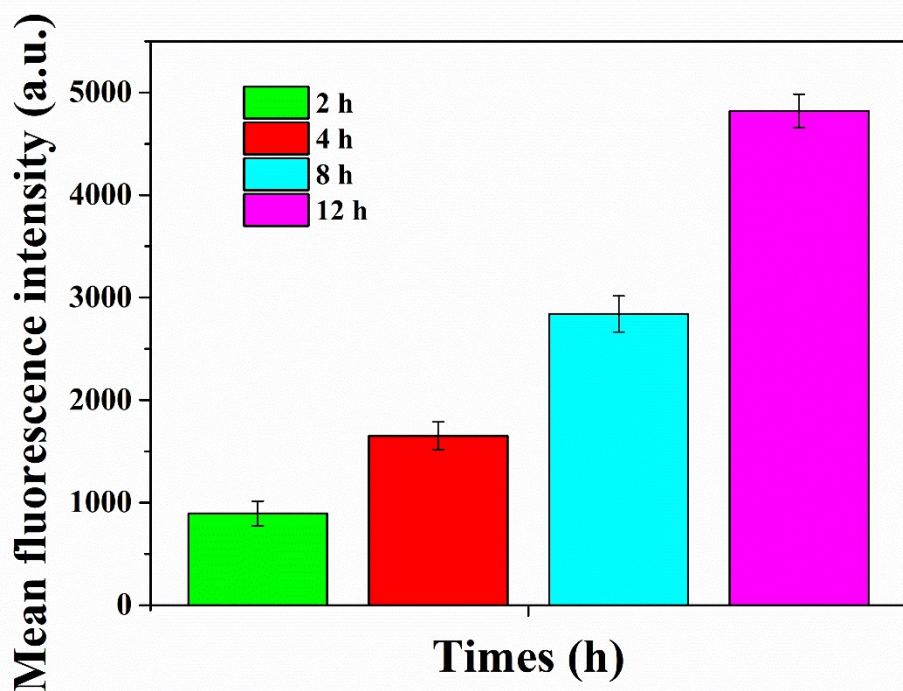


Fig. S15. Fluorescence intensity analysis of HeLa cells after treated with DOX/MSNs-PDA-HA for 2 h, 4 h, 8 h and 12 h measured by fluorescence spectrophotometer, respectively. Data are represented as mean \pm SD (n = 3).

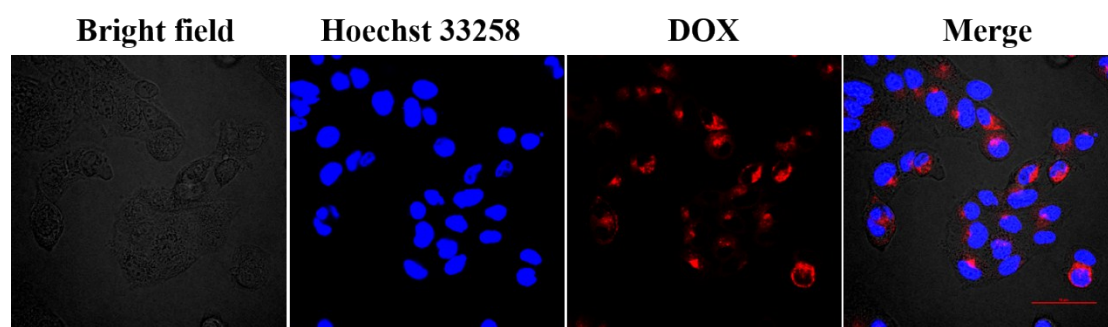


Fig. S16. CLSM images of L-02 cells after 12 h incubation with DOX/MSNs-PDA-HA (DOX concentration was equivalent to 1 $\mu\text{g}/\text{mL}$). Scale bar: 50 μm .

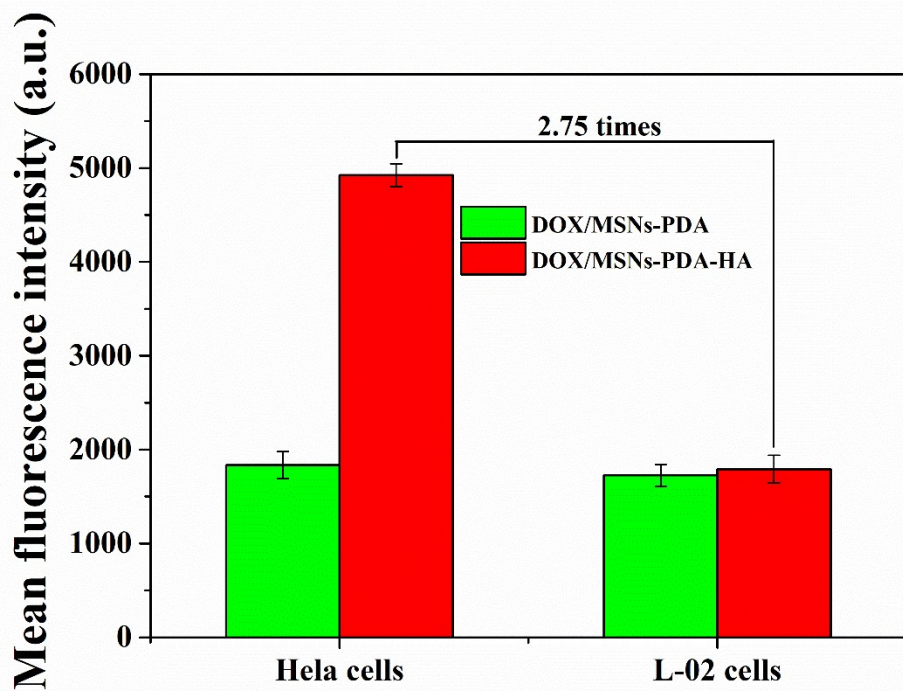


Fig. S17. Mean fluorescence intensity of DOX/MSNs-PDA and DOX/MSNs-PDA-HA endocytosed by HeLa and L-02 cells was measured by fluorescence spectrophotometer. Data are represented as mean \pm SD (n = 3).

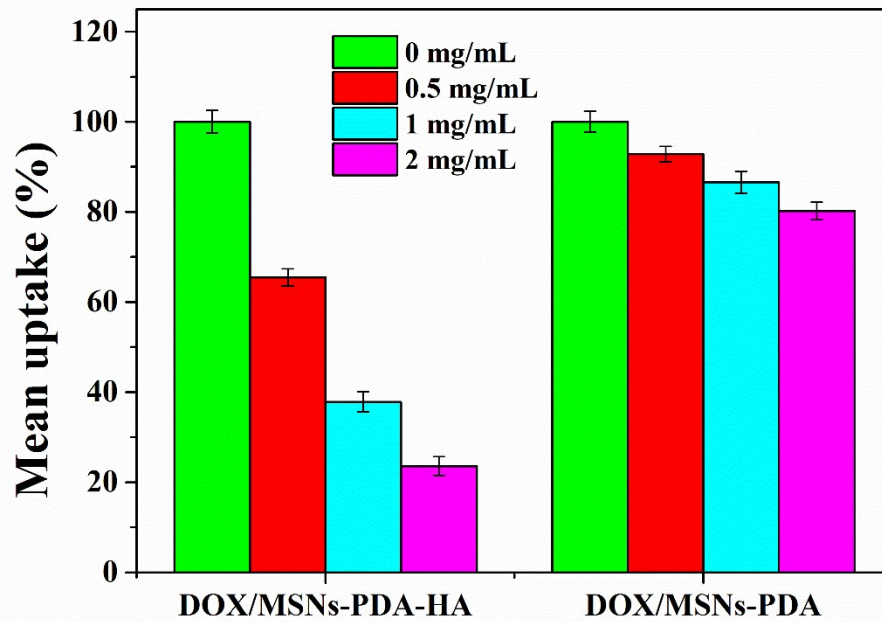


Fig. S18. Assessment of cell endocytosis mechanisms between cell and nanoparticles. HA competition inhibited cell specific particle endocytosis. Hela cell were cultured with particles after pre-treated with HA with different concentrations. Data are represented as mean \pm SD (n = 3).

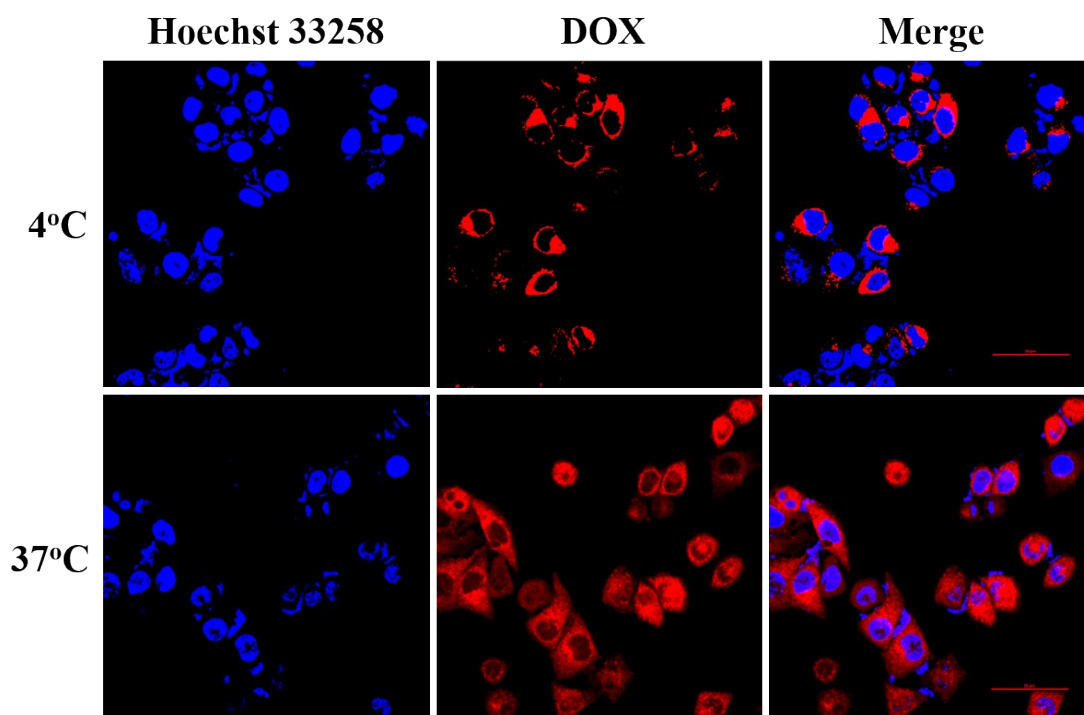


Fig. S19. Energy-dependent endocytosis behavior of DOX/MSNs-PDA-HA. CLSM images of HeLa cells treated with DOX/MSNs-PDA-HA at different temperatures (4 and 37°C).

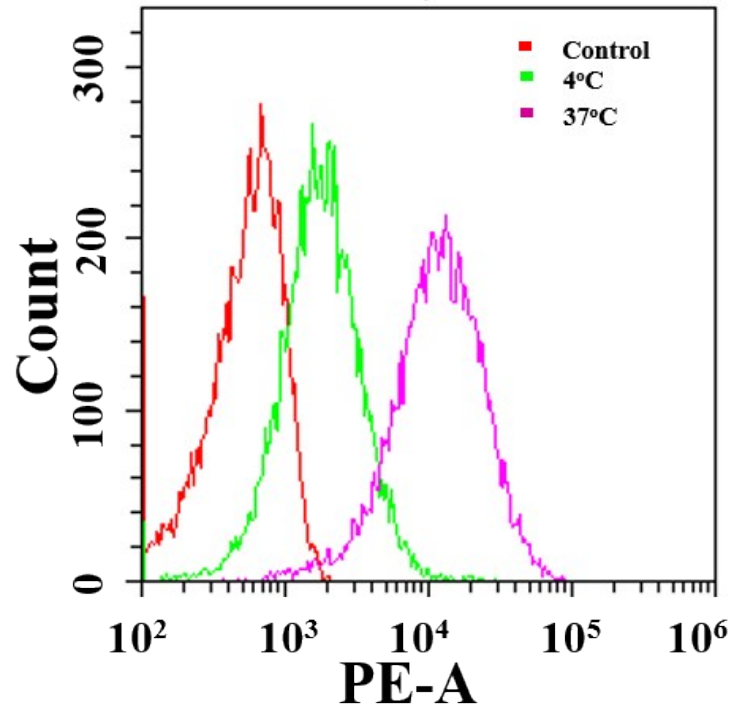


Fig. S20. Energy-dependent endocytosis behavior of DOX/MSNs-PDA-HA. Flow cytometry quantification of the cellular internalization of DOX/MSNs-PDA-HA against Hela cells at different temperatures (4 and 37°C).

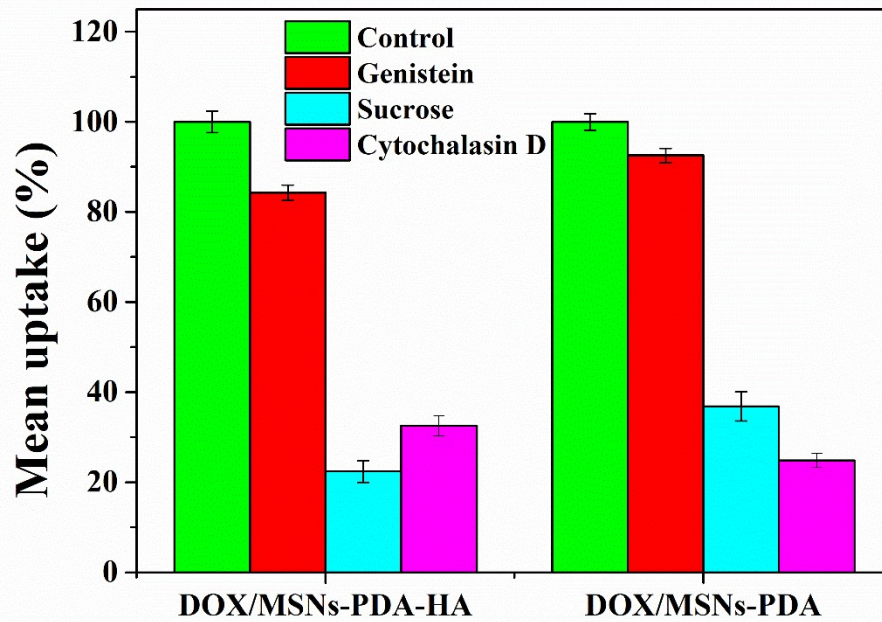


Fig. S21. Cell endocytosis mechanism assay. Uptake of nanoparticles by HeLa cells when pre-treated with Genistein, Sucrose and Cytochalasin D for 1 h before cultured with DOX/MSNs-PDA-HA and DOX/MSNs-PDA nanoparticles. Data are represented as mean \pm SD (n = 3).

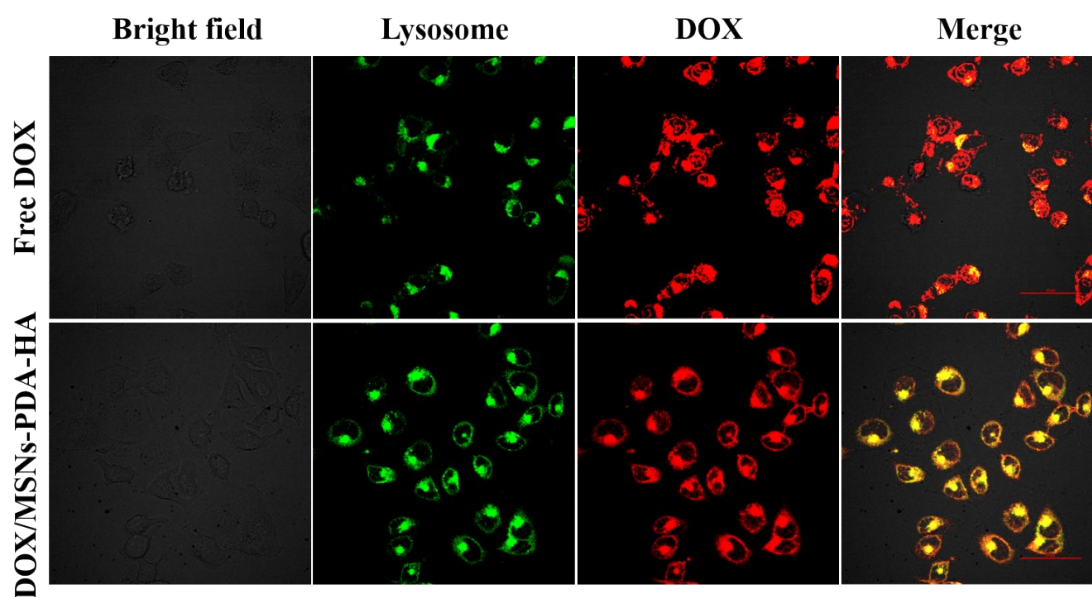


Fig. S22. CLSM images of HeLa cells after treated with free DOX and DOX/MSNs-PDA-HA for 12 h, while the cells labeled with lysosome (green). Scale bar: 50 μm .

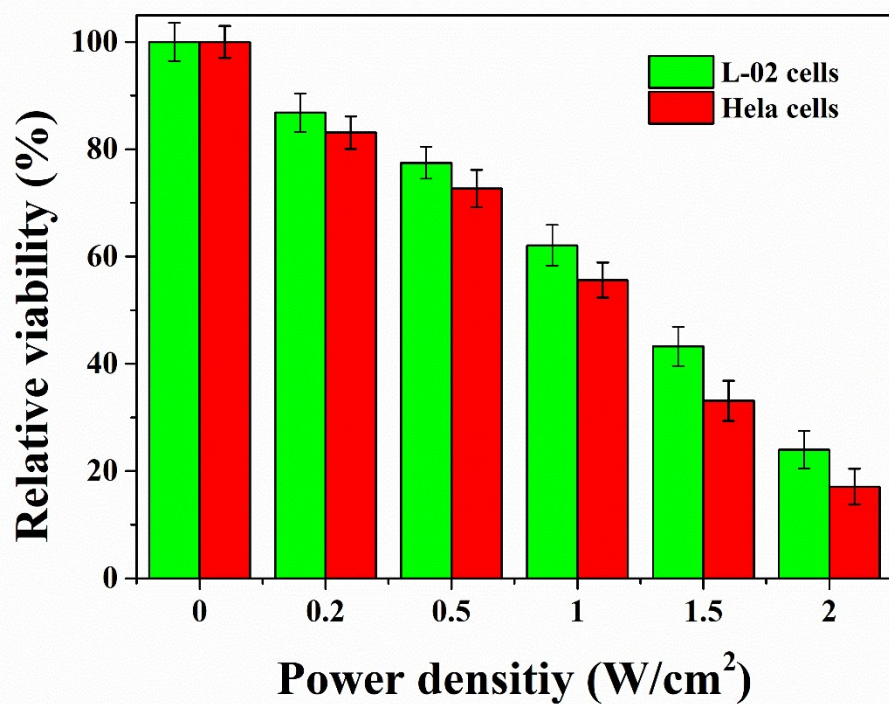


Fig. S23. Relative viabilities of L-02 and Hela cells incubated with MSNs-PDA-HA (100 $\mu\text{g}/\text{mL}$) after 5 min of 808 nm laser irradiation at different power densities for 24 h. Data are represented as mean \pm SD (n = 5).

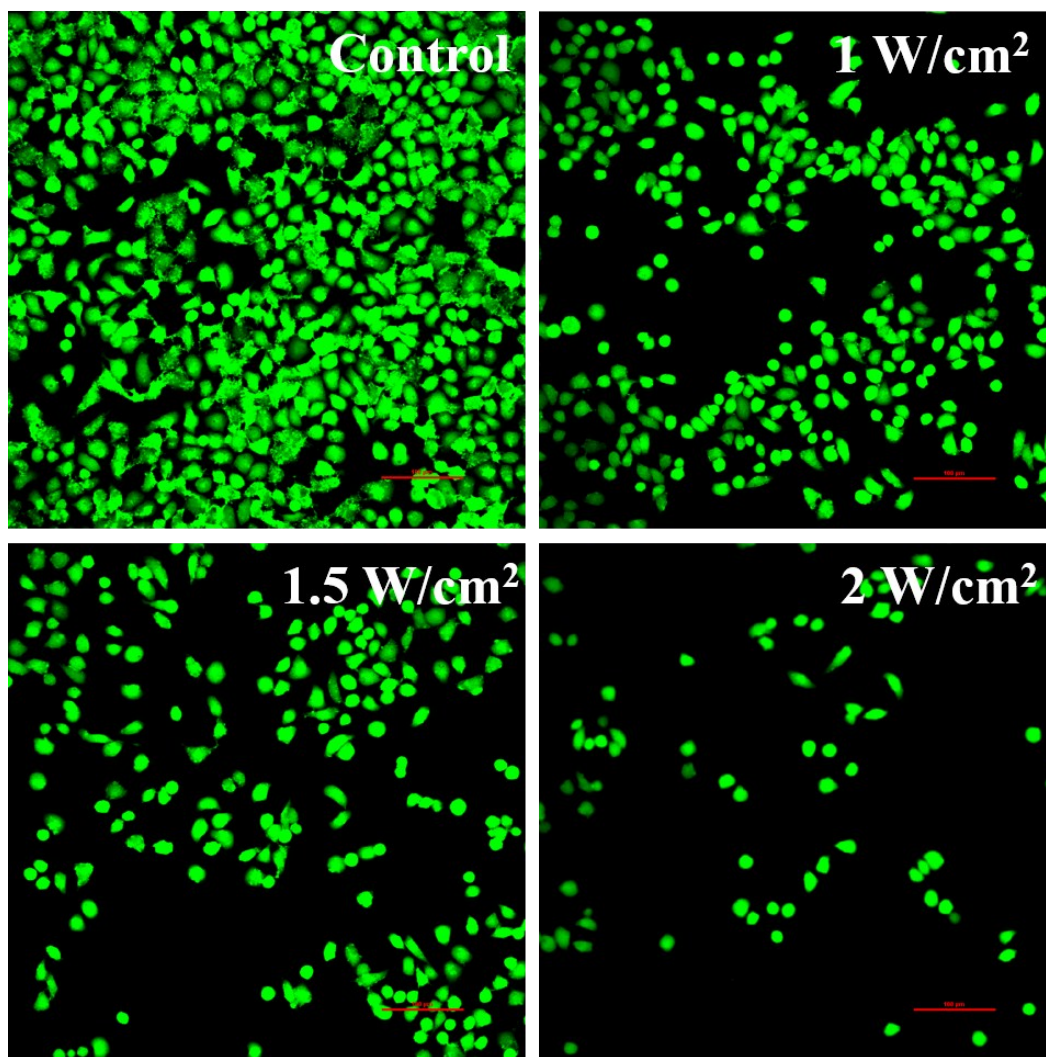


Fig. S24. Fluorescence images of calcein AM contained HeLa cells with MSNs-PDA-HA (100 $\mu\text{g}/\text{mL}$) incubation for 24 h with the 808 nm laser irradiation for 5 min at different power densities. Live cells stained by calcein AM, which displayed green colors.

Control



Free DOX



DOX/MSNs-PDA-HA



DOX/MSNs-PDA



DOX/MSNs-PDA-HA+NIR



Fig. S25. Representative photos of mice and tumors after treatment with PBS, free DOX, DOX/MSNs-PDA and DOX/MSNs-PDA-HA for 14 days with or without laser irradiation (808 nm irradiation, 10 min at 2.0 W/cm²).

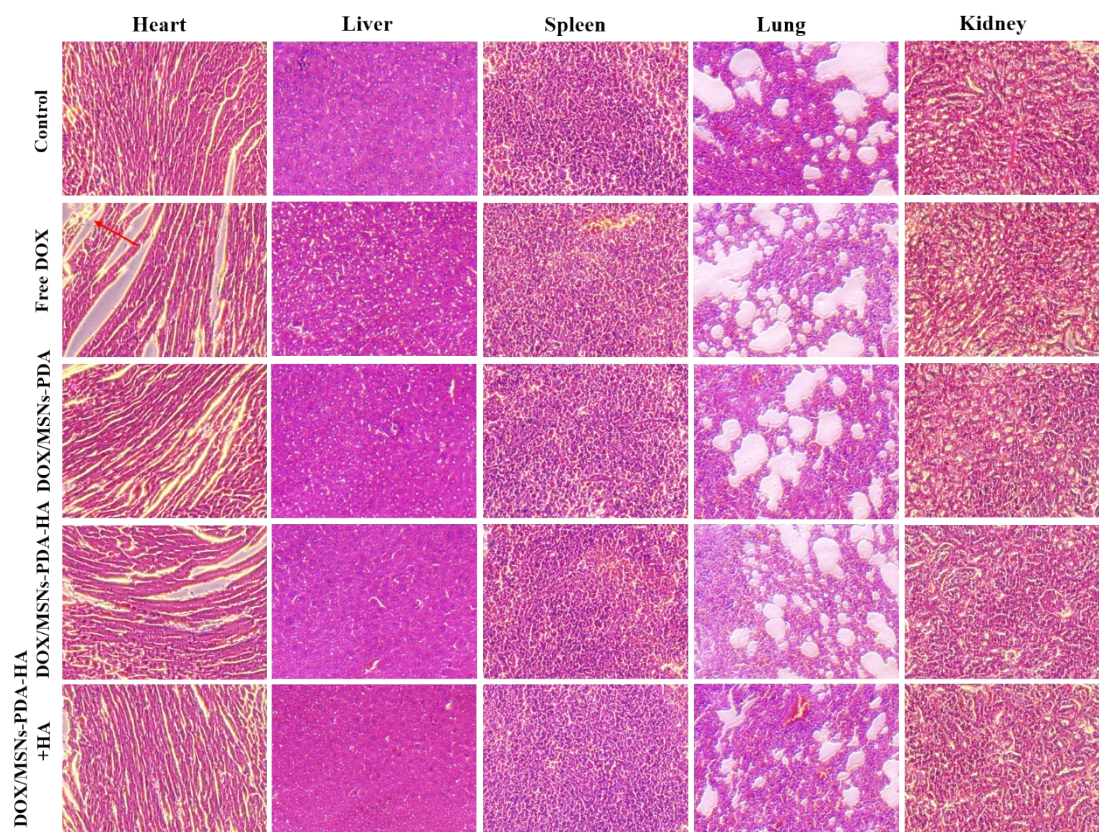


Fig. S26. Representative H&E sections of organ tissues (heart, liver, spleen, lung and kidney) of tumor-bearing BALB/c mice after treatment with PBS, free DOX, DOX/MSNs-PDA and DOX/MSNs-PDA-HA for 14 days with or without laser irradiation (808 nm irradiation, 10 min at 2.0 W/cm²).

Table S1. The hydrodynamic particle size distribution in water.

Samples	Size (nm)	PDI
MSNs	102.2 ± 3.6	0.104
MSNs-PDA	123.4 ± 5.3	0.116
MSNs-PDA-HA	169.3 ± 3.2	0.143

Table S2. Zeta potential results of MSNs before and after grafting with chemicals at each step.

Materials	Zeta Potential (mV)
MSNs	-23.4 ± 0.7
MSNs-PDA	-5.8 ± 0.6
MSNs-PDA-HA	-17.3 ± 0.4

Table S3. The surface functionalization extent of MSNs was characterized by TGA analysis and the final weight losses for all materials are presented in **Table S3**.

Materials	Final weight loss (wt %)
MSNs	4.73
MSNs-PDA	16.77
MSNs-PDA-HA	34.72

Table S4. The N₂ adsorption-desorption parameters of different functionalized MSN nanoparticles.

Sample	S_{BET} (m²/g)	V_{P} (cm³/g)	W_{BJH} (nm)
MSNs	902.51	0.503	2.7

MSNs-PDA	498.71	0.354	2.4
MSNs-PDA-HA	55.44	0.091	□2

References

[1] Zhao Q, Liu J, Zhu W, Sun C, Di D, Zhang Y, et al. Dual-stimuli responsive hyaluronic acid-conjugated mesoporous silica for targeted delivery to CD44-overexpressing cancer cells. *Acta Biomaterialia* 2015;23:147-156.

[2] He Q, Zhang J, Shi J, Zhu Z, Zhang L, Bu W, et al. The effect of PEGylation of mesoporous silica nanoparticles on nonspecific binding of serum proteins and cellular responses. *Biomaterials* 2010;31:1085-1092.